https://doi.org/10.5194/se-2020-146
Preprint. Discussion started: 28 September 2020

Solid Earth
Discussions
Open Access
EGU

Nano-scale earthquake records preserved in plagioclase microfractures from the lower continental crust

Arianne J. Petley-Ragan[1*], Oliver Plümper[2], Benoit Ildefonse[3], and Bjørn Jamtveit[1]

[1]Physics of Geological Processes, The Njord Centre, University of Oslo, Oslo, Norway

[2]Department of Earth Sciences, Utrecht University, Utrecht, The Netherlands

[3]Géosciences Montpellier, CNRS, University of Montpellier, Université des Antilles, Montpellier, France

Corresponding to: Arianne J. Petley-Ragan (a.j.petley-ragan@geo.uio.no)

Abstract. Seismic faulting causes wall rock damage driven by both mechanical stress and thermal energy. In the lower crust, coseismic damage has important implications for wall rock permeability, the progress of subsequent fluid-driven metamorphic reactions, and rock rheology. Wall rock microstructures reveal high-stress conditions near the slip surface during lower crustal earthquakes, however, there is limited documentation on the thermal effect. Here, we present a transmission electron microscopy study of coseismic microfractures in plagioclase feldspar from lower crustal granulites from the Bergen Arcs, Western Norway. Focused ion beam foils are collected 1.25 mm and 1.8 cm from a 2 mm thick eclogite facies pseudotachylyte vein. Dislocation-free plagioclase aggregates fill the microfractures and record a history of recovery from a short-lived high stress-temperature (σ-T) state caused by seismic slip and frictional melting along the nearby fault surface. The plagioclase aggregates retain the crystallographic orientation of the host rock and shape preferred orientation relative to the fault slip surface. We propose that plagioclase partially amorphized along the microfractures at peak stress conditions followed by repolymerization to form dislocation-free grain aggregates within the timeframe of pseudotachylyte formation. The heat from the slip surface dissipated into the wall rock causing a short-lived temperature peak. Subsequent cooling led to exsolution of intermediate plagioclase compositions by spinodal decomposition within a few millimeters distance to the fault surface. Our findings provide microstructural evidence for the high σ-T conditions that are expected in the proximity of seismic faults, highlighting the importance of micro- and nanostructures for the understanding of earthquakes ruptures.

1 Introduction

During continent-continent collisions, plagioclase-rich granulite- and amphibolite-facies rocks are strong, dry and prone to seismic faulting and subsequent metamorphism (Jamtveit et al., 2016). Plagioclase responds to lower crustal earthquakes by microfracturing and fragmentation followed by fluid- and stress-induced recrystallization (Mukai et al., 2014; Petley-Ragan et al., 2018; Soda and Okudaira, 2018). Grain size reduction by fracturing and subsequent recrystallization localizes strain in the lower crust, defining a transition from brittle to crystal-plastic deformation mechanisms with the potential to develop into shear zones (Svahnberg and Piazolo, 2010; Menegon et al., 2013; Okudaira et al., 2016; Marti et al., 2017). Thus, recrystallization and subsequent shear may overprint any microstructural record of the high-intensity stress conditions created by an earthquake. Analysis of plagioclase microstructures that have not undergone extensive annealing may provide valuable insight into the stress and temperature state experienced by the wall rock during a seismic event.

In a purely elastic model, Reches and Dewers (2005) showed that for a dynamic earthquake rupture propagating at 91% of the Rayleigh wave speed wall rock stresses may approach 10 GPa within 3 mm of a propagating rupture.

https://doi.org/10.5194/se-2020-146
Preprint. Discussion started: 28 September 2020

Solid Earth
Discussions
Open Access
EGU

Furthermore, for ambient lower crustal temperatures in the range 600-700°C, the transient temperature following an earthquake may exceed 1000°C within 1 cm of the slip surface (Bestmann et al., 2012; Clerc et al., 2018). Such conditions, although short-lived, are expected to drive irreversible processes within the rock record. Extensive wall rock fragmentation without shear strain around amphibolite and eclogite facies faults provide some evidence for the high stresses caused by the propagation of seismic ruptures (Austrheim et al., 2017; Petley-Ragan et al., 2019). Recent experimental studies have reported generation of amorphous material associated with fracturing and seismic slip under eclogite facies conditions (Incel et al., 2019). On the other hand, thermal radiation around frictional melt veins can drive recrystallization processes and form fine-grained dislocation-free aggregates (Bestmann et al., 2012; 2016). Signatures such as these could be beneficial in extracting rupture and melting properties of seismic faults.

Here we present a microstructural study of coseismic microfractures in plagioclase from granulites in the Bergen Arcs of Western Norway at varying distances to a lower crustal pseudotachylyte (Fig. 1a). Microfractures previously described by Petley-Ragan et al. (2018) were analyzed with a transmission electron microscope (TEM) equipped with an energy dispersive X-ray (EDX) detector to observe the mineralogy of fine-grained aggregates at the nanoscale. Our combined microstructural and chemical study aims at unravelling the thermo-mechanical evolution of plagioclase during and after earthquake rupture.

2 Geological Setting

The Lindås Nappe of the Bergen Arcs of Western Norway is host to a population of seismic faults identified by the presence of mm to cm thick pseudotachylytes that cut through granulite facies anorthosite (Austrheim and Boundy, 1994). The pseudotachylytes contain either an eclogite-facies or amphibolite-facies mineralogy, and the wall rock damage adjacent to them are spatially related to fine-grained products of the same metamorphic grade. The earthquakes took place within the lower crust during the Caledonian collision at 423-429 Ma (Jamtveit et al., 2019) and provoked fluid-driven amphibolitization at 600°C and 0.8-1.0 GPa (Jamtveit et al., 2018), and eclogitization at 650-750°C and 1.5-2.2 GPa (Jamtveit et al., 1990; Boundy et al., 1992; Glodny et al., 2008; Bhowany et al., 2017). The wall rock damage is best observed on the micro-scale due to the high density of microfractures (<50 µm thick) that criss-cross the wall rock mineral phases (Fig. 1b and c).

3 Plagioclase wall rock damage

Microfractures in wall rock plagioclase are found across the island of Holsnøy, adjacent to both types of pseudotachylytes, and their orientations are independent of the crystallographic orientation of the host grains. The microfractures contain fine-grained aggregates (grain size <5 µm) of dominantly plagioclase and K-feldspar (Fig. 1d and e). The grains within the microfractures have a crystallographic preferred orientation (CPO) that is controlled by the host plagioclase on either side of the microfracture (Fig. 2), and the K-feldspar grains have a CPO that mimics that of the plagioclase grains (Petley-Ragan et al., 2018). The grains also show a strong shape preferred orientation (SPO) with the long axis parallel to the pseudotachylyte wall (Fig. 2). Plagioclase compositions in the ranges An_{25-31} and An_{65-83} were measured in the microfractures. These originate from a host composition of An_{40} (Petley-Ragan et al., 2018). A similar bimodal range of plagioclase compositions were also observed at garnet-plagioclase phase boundaries and in an amphibolite facies micro-shear zone at Isdal ca. 40 km NE of Holsnøy (Mukai et al., 2014).

https://doi.org/10.5194/se-2020-146
Preprint. Discussion started: 28 September 2020

Solid Earth
Discussions
Open Access
EGU

The mineralogy of the microfractures and their associated reaction products varies locally. Some contain quartz and kyanite, while others are associated with intergrowths of clinozoisite, quartz and K-feldspar. Few microfractures contain minor amounts of carbonates or phengite. Microfracture mineralogy is found to depend on the X_{CO2} of the infiltrating fluid (Okudaira et al., 2016) and the orientation of the microfracture relative to the principle stress (Moore et al., 2019). The detailed evolution of the microfractures is thus dependent on a multitude of factors.

Two microfractures of dominantly plagioclase and K-feldspar previously described by Petley-Ragan et al. (2018) were subject to further study with transmission electron microscopy (TEM). The grain size distributions within these microfractures were characterized by electron backscatter diffraction (EBSD) (Aupart et al., 2018). The microfracture from Figure 1d will hereafter be referred to as Microfracture 1 (MF1) and is located 1.25 mm away from pseudotachylyte with a mean grain size of 1.73 μm^2 (Aupart et al., 2018). The microfracture from Figure 1d will be referred to as Microfracture 2 (MF2) and is located 1.8 cm away from the same pseudotachylyte (Fig. 1a) with a mean grain size of 2.14 μm^2 (Aupart et al., 2018). MF2 also contains a set of secondary fractures (Fig. 1c). Both microfractures are associated with clinozoisite, quartz and kyanite growth, and only MF2 contains dolomite. The lower J-index, greater misorientations and the presence of secondary fractures indicate that MF2 experienced more shear deformation than MF1 (Petley-Ragan et al., 2018).

4 Methods

Mass balance calculations were performed on three microfractures by comparing the bulk microfracture composition to the bulk host composition. Electron microprobe maps of the microfractures were obtained with a Cameca SX100 at the University of Oslo's Department of Geosciences. The mass balance was calculated in MATLAB. Focused ion beam (FIB) foils were prepared and TEM analyses were carried out at Utrecht University. The FEI Helios Nanolab G3 was used to cut FIB foils perpendicular to the length of the microfractures and ~15-20 µm in length in order to include both the host and microfracture constituents (Fig. 1d and e). The FEI Talos 200FX equipped with a high-sensitive 2D energy dispersive X-ray (EDX) system was used to obtain bright-field (BF), dark-field (DF) and high angular annual dark-field (HAADF) images in scanning TEM (STEM) mode. Large area EDX maps were acquired of the entire FIB foil for MF1 and parts of the FIB foil for MF2.

5 Results

Mass balance calculations based on three microfractures show that there is 5-11 times more K in the microfractures compared to the host composition (Fig. 3). A bright field TEM image shows that MF1 contains dislocation-poor and dislocation-free grains of dominantly plagioclase and K-feldspar defined by straight grain boundaries with 120° triple junctions (Fig. 4a). Few grains contain single dislocation walls within their centre. In contrast, the host plagioclase is lined with free dislocations that have formed a subgrain wall made up of closely spaced dislocations. Ankerite ($Ca(Fe,Mg)(CO_3)_2$), grossular-rich garnet and sphene are additional phases in MF1, with apatite and rutile inclusions inside the grains, pinned along grain boundaries and concentrated along the subgrain wall in the host (Fig. 4b).

The EDX map of MF1 displays homogeneous K-feldspar grains and plagioclase grains that are heterogeneous with respect to their CaAl and NaSi content (Fig. 4b). The K-feldspar grains are clustered together creating a fabric

https://doi.org/10.5194/se-2020-146
Preprint. Discussion started: 28 September 2020

dominated by grain boundaries instead of phase boundaries. The irregular composition distribution of Na and Ca in the plagioclase grains contradicts the backscatter electron image that suggests Ca zoning around the grains (Fig. 1d and 4b). Instead, the Ca-rich domains overlie areas with submicron lamellae (Fig. 5a-f). The lamellae are discontinuous throughout the plagioclase grains and, locally, they are superimposed by tapered mechanical twins (Fig. 5a). Other grains contain both lamellae and twins that are spatially distinct but are parallel to each other (Fig. 5d). In some grains, the lamellae appear slightly curved (Fig. 5c) while in others, the lamellae appear to form a 'tweed' structure (Fig. 5f). The spacing between lamellae is approximately 10-30 nm. Due to the high anorthite composition obtained for plagioclase within this microfracture (An_{65-83}; Petley-Ragan et al., 2018) this structure lies within the Bøggild-Huttenlocher miscibility gap (Smith and Brown, 1988; McConnell, 2008). The intergrowth is not observed within the host plagioclase.

MF2 is similarly dominated by dislocation-poor grains of plagioclase and K-feldspar with a number of grains displaying twinning (Fig. 6a). The twins of separate grains are approximately parallel to each other and to (010) of the host plagioclase (see Fig. 6 of Petley-Ragan et al., 2018), reinforcing the preservation of crystallographic orientations of the host through the fracturing and recovery process. Kyanite and a K-rich micaceous phase are additional phases in MF2. Apatite inclusions are present within the grains and pinned along grain boundaries. The fabric is defined by 120° triple junctions with rare dislocation-rich grains that display irregular boundaries (Fig. 6b).

The EDX map of MF2 shows clustered homogeneous K-feldspar grains and zoned plagioclase grains (Fig. 6c) creating again a grain boundary-dominated fabric. Unlike MF1, the plagioclase grains in MF2 display Ca-enrichment at their grain boundaries and the submicron lamellae are absent. The Ca-rich rims are approximately 100-200 nm thick.

6 Discussion

The microfractures offer insight into the evolution of plagioclase feldspar that resulted from the high stress and high-temperature environment created near an earthquake slip plane. The dislocation-free nature of almost all grains in MF1 and MF2 suggest nearly complete annealing of the material within the microfractures (Fig. 4a and 6a). The grain fabric is dominated by straight phase and grain boundaries, 120° triple junctions and pinned apatite inclusions suggesting the migration of grain boundaries. The inheritance of the crystallographic orientation of the host plagioclase and its twins within the grains, furthermore, points towards an initial annealing process that is able to transfer and preserve crystallographic information (Passchier and Trouw, 2005). An equilibrium fabric with crystallographic inheritance is generally created by dislocation creep and grain boundary migration (Passchier and Trouw, 2005). However, the parallel shape preferred orientation of the grains to the pseudotachylyte wall suggests that annealing was initiated while a stress or thermal field generated by the seismic slip was still present (Petley-Ragan et al., 2018). This constrains the time scale of microfracture annealing to the duration of pseudotachylyte crystallization and cooling (seconds to minutes). Dislocation- and grain boundary migration are too slow to have taken place within this time scale, and it is additionally puzzling as to why these mechanisms were not active within the dislocation-rich host. Thus, we postulate that a much more rapid recrystallization process took place prior to grain boundary migration and final annealing within the microfractures, and this process must have been focused and enhanced by local factors such as fluid infiltration and heat from the nearby pseudotachylyte. The resulting grain

https://doi.org/10.5194/se-2020-146
Preprint. Discussion started: 28 September 2020


Solid Earth
Discussions
Open Access
EGU

size distributions as discussed by Aupart et al. (2018) furthermore show striking deviations from a steady-state distribution.

6.1 Stressed wall rock plagioclase

Deformation experiments performed at eclogite facies conditions may offer some insight into the microstructures that were present in the microfractures before complete recovery. Incel et al. (2017; 2019) observed brittle fractures filled with amorphous material during deformation experiments on blueschist under eclogite facies conditions. They interpret the amorphous material to result from shock loading during the propagation of a dynamic rupture. Although their experiments involved a short recovery time (<1 hour) some of the amorphous material recrystallized, creating idiomorphic garnet crystals with a size of ~20 nm.

The amorphization of plagioclase feldspar is dependent on pressure (P), temperature (T), composition (X), compression rate (P/t) and pressure duration (t). Amorphization that is strongly dependent on temperature is commonly referred to as heterogeneous amorphization or melting, and is a relatively slow process due to its dependence on the diffusion of atoms (Wolf et al., 1990). On the other hand, amorphization that is strongly dependent on pressure is referred to as pressure-induced amorphization, which may be static or dynamic, depending on the compression rate (Sharma and Sikka, 1996). For the following, the pressure-induced amorphization of plagioclase will be discussed. For anorthite-rich compositions (An_{51-100}) complete pressure-induced amorphization occurs $P \geq 13$ GPa and T = 660°C, while albite-rich (An_2) compositions are not completely amorphous until $P \geq 26$ GPa and T = 950°C (Daniel et al., 1997; Kubo et al., 2009; Tomioka et al., 2010). Furthermore, short pressure durations result in lower degrees of amorphization (Tomioka et al., 2010) while high compression rates of 10^1-10^2 GPa/s can reduce the pressure required for amorphization (Sims et al., 2019). The short-lived (microseconds) high intensity (10^6 GPa/s) conditions in the proximity of earthquake rupture tips (Reches and Dewers, 2005) may partially amorphize plagioclase feldspar (An_{40}) in the wall rock, even if the local pressure for *complete* amorphization is not reached. The presence of asymmetric tensile cracks on some of the microfractures indicates that the propagation velocity of the microfractures approached the shear wave velocity (Petley-Ragan et al., 2018) inducing similar short-lived high-intensity stresses within their vicinity. Therefore, a mixture of amorphous material with remnant fragments may have been present within the microfractures immediately after earthquake and microfracture rupture.

Repolymerization of amorphous material on the microfracture walls and remnant fragments would directly transfer the crystallographic orientation of the host. Crystallographic information may also be preserved by the presence of short-range atomic order within amorphous material, allowing for immediate repolymerization without the aid of a fragment nucleus (Casey et al., 1993; Konrad-Schmolke et al., 2018). Repolymerization has also been suggested to occur directly along crystal lattice defects where amorphous material originates (Konrad-Schmolke et al., 2018). In this context, dislocations within the grains may have healed much more quickly than would be expected from dislocation migration recrystallization and the fragments would have experienced healing from multiple available interfaces. Other preferred areas of repolymerization were likely parallel to the minimum principal stress direction, growing grains with a stress-dependent SPO. Therefore, recrystallization from an amorphous material may be a likely candidate to create the observed dislocation-free fabric with a strong SPO within the timeframe of pseudotachylyte formation.

https://doi.org/10.5194/se-2020-146
Preprint. Discussion started: 28 September 2020

6.2 Cooling within the vicinity of pseudotachylyte

The nano-scale intergrowth within the plagioclase grains from MF1 is here interpreted as exsolution lamellae that formed as a result of rapid cooling from high temperatures within the vicinity of the pseudotachylyte. Similar intergrowths were found in what is called the 'complex feldspar', a microstructure of fragmented plagioclase first described in an amphibolite facies shear zone at Isdal, approximately 40 km east of Holsnøy (Mukai et al., 2014). They interpreted the structure as fluid- and stress-induced coarsening of exsolution lamellae. Although plausible, this would require that plagioclase exsolution occurred prior to the stress and thermal anomaly created by the earthquake. No intergrowths are observed within the host plagioclase in the present study, and it is unlikely that diffusion rates were high enough to form lamellae within the dry granulite. Our documentation of the exsolution lamellae within plagioclase grains from the microfracture nearest the pseudotachylyte (Fig. 1a) suggests that the thermal anomaly produced by the frictional melt vein affected the intracrystalline structure of the plagioclase grains.

Intergrowths form when plagioclases of intermediate composition cool from high temperature and enter a miscibility gap below 800°C, exsolving into separate calcic and sodic regions (Carpenter, 1994; McConnell, 2008). Although the ambient eclogite facies conditions (650-750°C) place the plagioclase within the miscibility gap, the absence of fluids hinders chemical diffusion and thus exsolution. It is only until after an earthquake causes wall rock damage that fluids enter the wall rock through coseismic microfractures, and these fluids are likely overheated by the frictional slip (Bestmann et al., 2016). Simultaneously, the wall rock within <1 cm of the pseudotachylyte experiences a thermal anomaly before rapidly cooling back to ambient conditions at rates on the order of a few °C/s (Bestmann et al., 2012). NaSi-CaAl diffusivity in plagioclase at 900-1000°C is ~10^{-15} cm^2/s (K[illegible]uk and Lepezin, 2009). Assuming that elevated temperatures lasted for up to a minute within 1 mm of the pseudotachylyte (MF1), diffusion would be efficient over a distance of 25 nm, similar to the spacing of lamellae observed (Fig. 5). At distances greater than 1 cm from the pseudotachylyte (MF2), the wall rock experiences minor heating to a few 10°C above ambient. Therefore, rapid cooling from elevated temperatures back to ambient conditions and into the miscibility gap only took place within close proximity to the pseudotachylyte.

7 Conclusion

Our nanostructural observations are relevant for understanding plagioclase deformation during and after an earthquake in the lower crust, prior to any subsequent shear zone development. We propose that plagioclase within the microfractures experienced partial amorphization at peak pressures coeval with earthquake propagation and microfracturing in the wall rock. Repolymerization on microfracture walls, remnant fragments, dislocations and from short-range atomic ordering in the direction parallel to the minimum principal stress formed a strong CPO and SPO in the grains. Repolymerization and recrystallization within the timeframe of pseudotachylyte formation explain the presence of dislocation-free grains, as has been interpreted for similar structures observed in quartz (Bestmann et al., 2012). In close proximity to the pseudotachylyte, wall rock temperatures reached 900-1000°C before rapidly cooling back to ambient eclogite facies conditions and into the plagioclase miscibility gap. This caused exsolution of intermediate plagioclase compositions and formation of nano-scale lamellae. We hypothesize that the lamellae described here are a unique signature of rapid cooling within plagioclase-rich wall rock in the vicinity of pseudotachylyte. A study of a larger number of plagioclase microfractures at varying distances to pristine pseudotachylyte would provide more information and constraints on the occurrence of these intergrowths.

https://doi.org/10.5194/se-2020-146
Preprint. Discussion started: 28 September 2020

The dependence of plagioclase microstructures on temperature and cooling rate and their sensitivity to fluid interaction offers a new tool for unraveling the history of wall rocks and their associated earthquakes.

Data and Sample Availability

Raw electron backscatter diffraction and geochemical data are available on Open Science Framework at osf.io/g36m7/. Rock samples are available through A. P.-R. and FIB foils are available through O. P.

Author Contribution

B. J. designed the project. A. P.-R. collected the samples, obtained and analyzed the EBSD and geochemical data. B. I. helped collect and interpret the EBSD data. O. P. cut the FIB foils, and obtained and interpreted the TEM images. A.P.-R., O. P. and B. J. were part of discussions. A. P.-R. and B. J. wrote the manuscript.

Competing Interests

The authors declare that they have no conflict of interest.

Acknowledgements

This project was supported by the European Research Council (ERC) Advanced Grant Agreement 669972, "Disequilibrium Metamorphism" ("DIME") to B. J., and the Natural Science and Engineering Research Council (NSERC) of Canada Postgraduate Scholarship Doctoral (PGS-D) 489392 to A. P.-R. O. P. has been supported by an ERC Starting Grant "nanoEARTH" (852069). We thank H. Austrheim for field guidance on Holsnøy and hospitality in Western Norway. We thank X. Zhong for help with the mass balance calculations, F. Barou for assistance with EBSD measurements and M. Erambert for help on the electron microprobe.

References

Austrheim, H. and Boundy, T. M.: Pseudotachylytes generated during seismic faulting and eclogitization of the deep crust, Science, 265, 82-83, http://www.jstor.org/stable/2884364, 1994.

Austrheim, H., Dunkel, K. G., Plümper, O., Ildefonse, B., Liu, Y., and Jamtveit, B.: Fragmentation of wall rock garnets during deep crustal earthquakes, Sci. Adv., 3, 1-8, https://doi.org/10.1126/sciadv.1602067, 2017.

Bestmann, M., Pennacchioni, G., Nielsen, S., Göken, M., and de Wall, H.: Deformation and ultrafine dynamic recrystallization of quartz in pseudotachylyte-bearing brittle faults: A matter of a few seconds. J. Struct. Geol., 38, 21-38, https://doi.org/10.1016/j.jsg.2011.10.001, 2012.

Bestmann, M., Panncchioni, G., Mostefaoui, S., Göken, M. and de Wall, H.: Instantaneous healing of micro-fractures during coseismic slip: Evidence from microstructure and Ti in quartz geochemistry within an exhumed pseudotachylyte-bearing fault in tonalite, Lithos, 254-255, 84-93, https://doi.org/10.1016/j.lithos.2016.03.011, 2016.

Bhowany, K., Hand, M., Clark, C., Kelsey, D. E., Reddy, S. M., Pearce, M. A., Tucker, N. M., and Morrissey, L. J.: Phase equilibria modelling constraints on P-T conditions during fluid catalysed conversion of granulite to eclogite in the Bergen Arcs, Norway, J. Metamorph. Geol., https://doi.org/10.1111/jmg.12294, 2017.

https://doi.org/10.5194/se-2020-146
Preprint. Discussion started: 28 September 2020


Solid Earth
Discussions
Open Access
EGU

Boundy, T.M., Fountain, D.M., and Austrheim, H.: Structural development and petrofabrics of eclogite facies shear zones, Bergen Arcs, western Norway: implications for deep crustal deformational processes, J. Metamorph. Geol., 10, 2, 127-146, https://doi.org/10.1111/j.1525-1314.1992.tb00075.x, 1992.

Carpenter, M. A.: Mechanisms and kinetics of Al-Si ordering in anorthite: I. Incommensurate structure and domain coarsening, Am. Mineral., 76, 1110-1119, 1991.

Casey, W. H., Westrich, H. R., Banfield, J. F., Ferruzi, G. and Arnold, G. W.: Leaching and reconstruction at the surfaces of dissolving chain-silicate minerals, Nature, 366, 253-256, https://doi.org/10.1038/366253a0, 1993.

Daniel, I., Gillet, P., McMillan, P. F., Wolf, G. and Verhelst, M. A.: High-pressure behavior of anorthite: Compression and amorphization. J. Geophys. Res., 102, 10313-10325. https://doi.org/10.1029/97JB00398, 1997.

Glodny, J., Kühn, A., and Austrheim, H.: Geochronology of fluid-induced eclogite and amphibolite facies metamorphic reactions in subduction-collision system, Bergen Arcs, Norway, Contrib. Mineral. Petr., 156, 1, 27-48, https://doi.org/10.1007/s00410-007-0272-y, 2008.

Incel, S., Hilairet, N., Labrousse, L., John, T., Deldicque, D., Farrand, T., Wang, Y., Renner, J., Morales, L. and Schubnel, A.: Laboratory earthquakes triggered during eclogitization of lawsonite-bearing blueschist. Earth Planet. Sci. Lett., 459, 320-331, https://doi.org/10.1130/G45527.1, 2017.

Incel, S., Labrousse, L., Hilairet, N., John, T., Gasc, J., Shi, F., Wang, Y., Andersen, Renard, F., Jamtveit, B. And Schubnel, A.: Reaction induced embrittlement of the lower continental crust, Geology, 47, 3, 235-238, https://doi.org/10.1130/G45527.1, 2019.

Jamtveit, B., Austrheim, H., and Putnis, A.: Disequilibrium metamorphism of stressed lithosphere, Earth Sci. Rev., 154, 1-13. https://doi.org/10.1016/j.earscirev.2015.12.002, 2016.

Jamtveit, B., Bucher-Nurminen, K. and Austrheim, H.: Fluid controlled eclogitization of granulites in deep crustal shear zones, Bergen Arcs, Western Norway, Contrib. Mineral Petr., 104, 184-193, https://doi.org/10.1007/BF00306442, 1990.

Jamtveit, B., Moulas, E. Andersen, T. B., Austrheim, H., Corfu, F., Petley-Ragan, A. and Schmalholz, S. M.: High pressure metamorphism caused by fluid induced weakening of deep continental crust. Sci. Rep., 8, 17011, https://doi.org/10.1038/s41598-018-35200-1, 2018.

Jamtveit, B., Petley-Ragan, A., Incel, S., Dunkel K. G., Aupart, C., Austrheim, H., Corfu, F., Menegon, L. and Renard, F.: The effects of earthquakes and fluids on the metamorphism of the lower continental crust, J. Geophys. Res., 124, 8, 7725-7755, https://doi.org/10.1029/2018JB016461, 2019.

Konrad-Schmolke, M., Halama, R., Wirth, R., Thomen, A., Klitscher, N., Morales, L., Schreiber, A. and Wilke, F. D. H.: Mineral dissolution and reprecipitation mediated by an amorphous phase, Nature contrib., 9, https://doi.org/10.1038/s41467-018-03944-z, 2018.

Kubo, T., Kimura, M., Kato, T., Nishi, M., Tominaga, A., Kikegawa, T. and Funakoshi, K.: Plagioclase breakdown as an indicator for shock conditions of meteorites, Nat. Geosci., 3, 41-45, https://doi.org/10.1038/ngeo704, 2009.

Marti, S., Stünitz, H., Heilbronner, R., Plümper, O. and Drury, M.: Experimental investigation of the brittle-viscous transition in mafic rocks – Interplay between fracturing, reaction, and viscous deformation, J. Struct. Geol, 105, 62-79, https://doi.org/10.1016/j.jsg.2017.10.011, 2017.

https://doi.org/10.5194/se-2020-146
Preprint. Discussion started: 28 September 2020


Solid Earth
Discussions
Open Access
EGU

McConnell, J.: The origin and characteristics of incommensurate structures in the plagioclase feldspars, Can. Mineral., 46, 1389-1400, https://doi.org/10.3749/canmin.46.6.1389, 2008.

Menegon, L., Stünitz, H., Nasipuri, P., Heilbronner, R. and Svahnberg, H.: Transition from fracturing to viscous flow in granulite facies perthitic feldspar (Lofoten, Norway), J. Struct. Geol., 48, 95-112, https://doi.org/10.1016/j.jsg.2012.12.004, 2013.

Moore, J., Beinlich, A., Austrheim, H. and Putnis, A.: Stress orientation-dependent reactions during metamorphism, Geology, 47, 1-4, https://doi.org/10.1130/G45632.1, 2019.

Mukai, H., Austrheim, H., Putnis, C. V., and Putnis, A.: Textural evolution of plagioclase feldspar across a shear zone: Implications for deformation mechanism and rock strength, J. Petrol., 55, 1457-1477, https://doi.org/10.1093/petrology/egu030, 2014.

Okudaira, T., Shigematsu, N., Harigane, Y., and Yoshida, K.: Grain size reduction due to fracturing and subsequent grain-size-sensitive creep in lower crustal shear zone in the presence of a CO2-bearing fluid, J. Struct. Geol., 95, 171-187, https://doi.org/10.1016/j.jsg.2016.11.001, 2016.

Petley-Ragan, A., Dunkel, K. G., Austrheim, H., Ildefonse, B. and Jamtveit, B.: Microstructural records of earthquakes in the lower crust and associated fluid-driven metamorphism in plagioclase-rich granulites. J. Geophys. Res.-Sol Ea., 123, 1-18, https://doi.org/10.1029/2017JB015348, 2018.

Petley-Ragan, A., Ben-Zion, Y., Austrheim, H., Ildefonse, B., Renard, F. and Jamtveit B.: Dynamic earthquake rupture in the lower crust, Sci. Adv., 5, https://doi.org/10.1126/sciadv.aaw0913, 2019.

Passchier, C., and Trouw, R.: Microtectonics. Springer, Berlin., 2005.

Reches, Z. and Dewers, T. A.: Gouge formation by dynamic pulverization during earthquake rupture, Earth Planet. Sc. Lett., 235, 361-374, https://doi.org/10.1016/j.epsl.2005.04.009, 2005.

Sharma, S. and Sikka, S.: Pressure Induced Amorphization of Materials, Progress in Materials Science, 40, 1-77, 1996.

Sims, M., Jaret, S. J., Carl, E.-R., Rhymer, B., Schrodt, N., Mohrholz, V., Smith, J., Konopkova, Z., Liermann, H.-P., Glotch, T. D. and Ehm, L.: Pressure-induced amorphization in plagioclase feldspars: A time-resolved powder diffraction study during rapid compression, Earth Planet Sc. Lett., 507, 166-174, https://doi.org/10.1016/j.epsl.2018.11.038, 2019.

Smith, J. V. and Brown, W. L.: Feldspar Minerals, vol. 1, Springer, Berlin, 1988.

Soda, Y. and Okudaira, T.: Microstructural evidence for the deep pulverization in a lower crustal meta-anorthosite, Terra Nova, 1-7, https://doi.org/10.1111/ter.12355, 2018.

Svahnberg, H. and Piazolo, S.: The initiation of strain localisation in plagioclase-rich rocks: Insights from detailed microstructural analyses, J. Struct. Geol, 32, 1404-1416, https://doi.org/10.1016/j.jsg.2010.06.011, 2010.

Tomioka, N., Kondo, H., Kunikata, A. and Nagai, T.: Pressure-induced amorphization of albitic plagioclase in an externally heated diamond anvil cell, Geophys. Res. Lett., 37, 1-5, https://doi.org/10.1029/2010GL044221, 2010.

Wolf, D., Okamoto, P., Yip, S., Lutsko, J. F. and Kluge, M.: Thermodynamic parallels between solid-state amorphization and melting, J. Material Res., 5, 286-301, https://doi.org/10.1557/JMR.1990.0286, 1990.

https://doi.org/10.5194/se-2020-146
Preprint. Discussion started: 28 September 2020

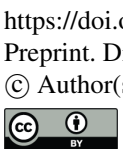

Solid Earth
Discussions
Open Access
EGU

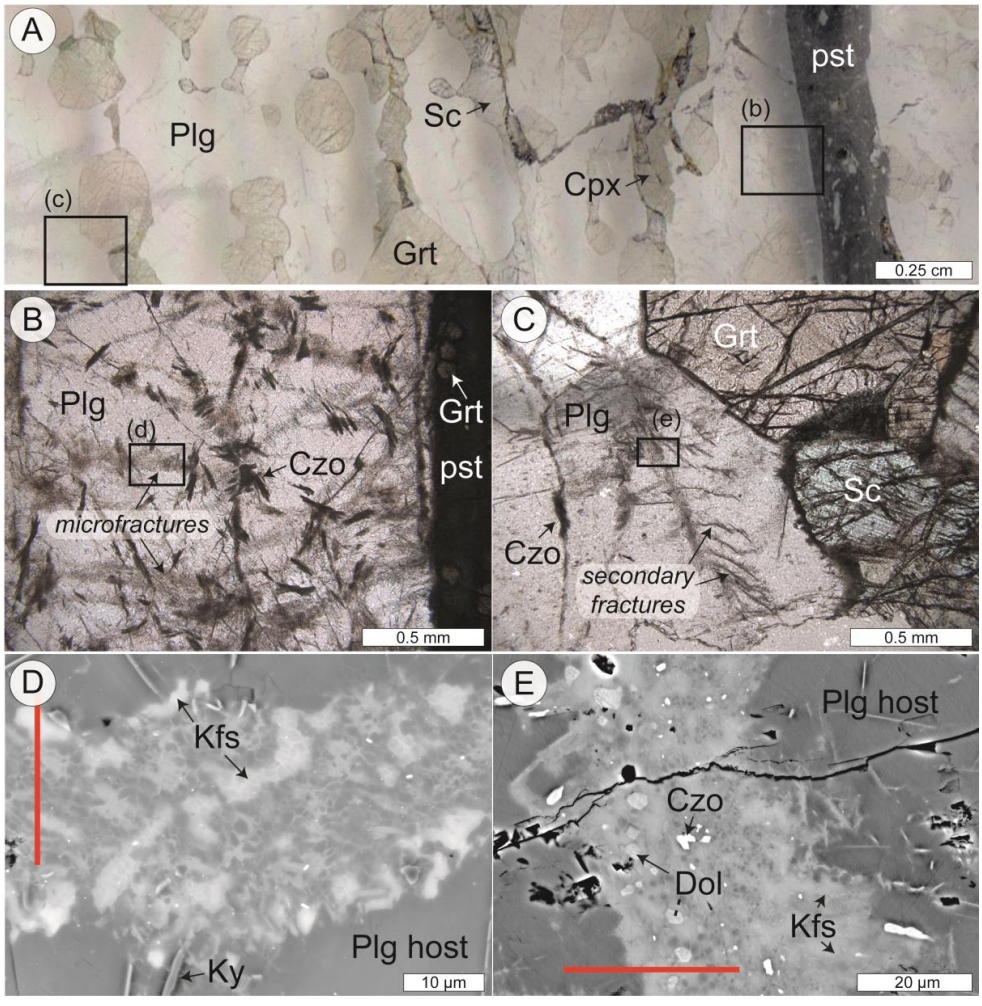

Figure 1: Fractured wall rock plagioclase. (a) Thin section scan of wall rock plagioclase (Plg), garnet (Grt), clinopyroxene (Cpx) and scapolite (Sc) adjacent to an eclogite facies pseudotachylyte (pst) on Holsnøy. **(b)** Fine-grained reaction products of clinozoisite (Czo) are associated with the microfractures. Box denotes the location of MF1. **(c)** Some microfractures in plagioclase display secondary cracking. Box denotes the location of MF2. **(d)** Backscatter electron image of MF1 with fine-grained plagioclase, alkali feldspar (Kfs) and minor kyanite (Ky). **(e)** Backscatter electron image of MF2 with fine-grained plagioclase, K-feldspar, dolomite (Dol) and clinozoisite. Red lines indicate the location of focused ion beam cuts for TEM analysis shown in Figs. 4-6.

https://doi.org/10.5194/se-2020-146
Preprint. Discussion started: 28 September 2020

Solid Earth
Discussions
Open Access
EGU

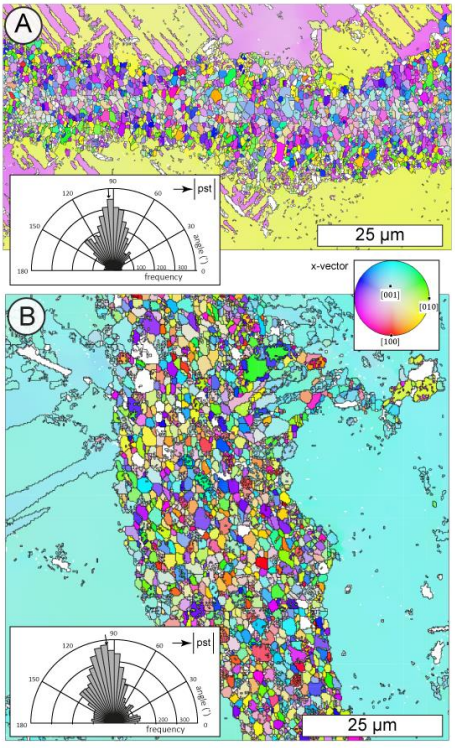

Figure 2: Crystallographic orientations of the grains within the microfractures. (a) Inverse pole figure coloring orientation map of MF1 with inset of grain SPO. **(b)** Orientation map of MF2 with inset of grain SPO. Modified after Petley-Ragan et al. (2018).

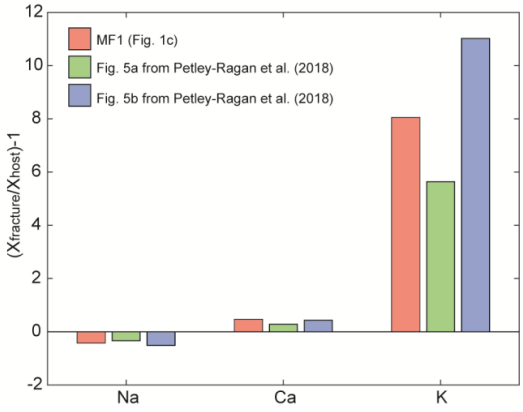

Figure 3: Mass balance of plagioclase microfractures. Three separate plagioclase microfractures were analyzed for Na, Ca and K. $X_{fracture}$ is the bulk composition of the fracture and X_{host} is the bulk composition of the adjacent plagioclase host.

https://doi.org/10.5194/se-2020-146
Preprint. Discussion started: 28 September 2020

Solid Earth
Discussions
Open Access
EGU

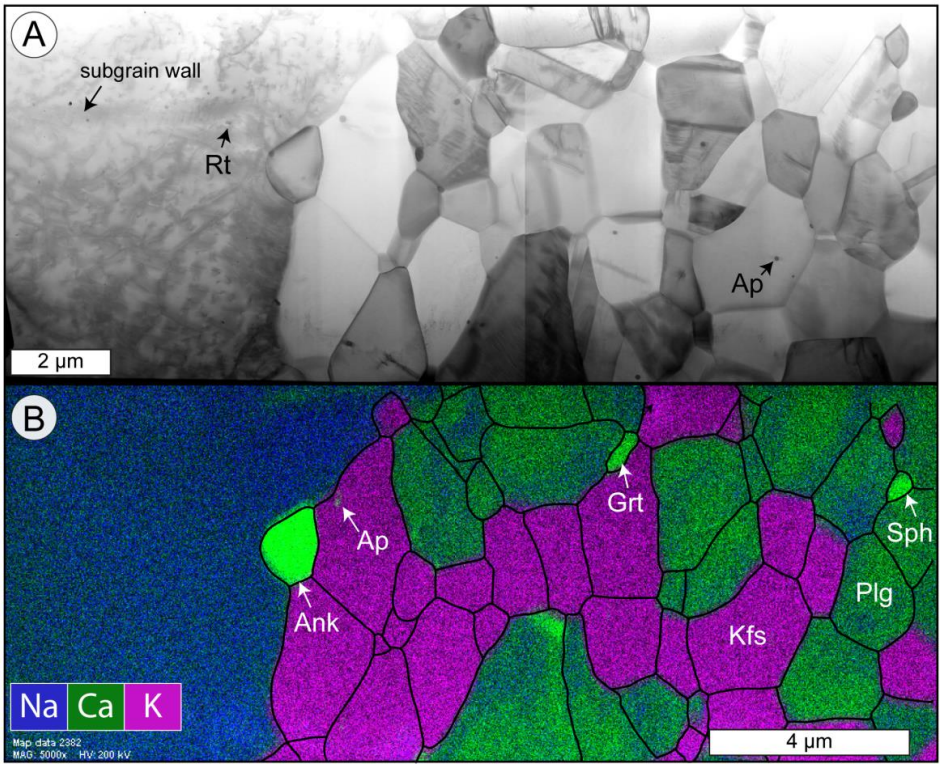

353

354 **Figure 4: Microstructures of MF1. (a)** BF-STEM image of the entire FIB cut from Fig. 1d. The plagioclase (Plg)
355 host to the left is rich in dislocations while the grains within the microfracture to the right are poor to absent of
356 dislocations. Apatite (Ap) and rutile (Rt) inclusions are present within the host and the grains, as well as pinned
357 along grain boundaries in the microfracture. **(b)** EDX map overlain with grain and phase boundaries (black).
358 Ankerite (Ank), garnet (Grt) and sphene (Sph) are additional phases within the microfracture.

https://doi.org/10.5194/se-2020-146
Preprint. Discussion started: 28 September 2020

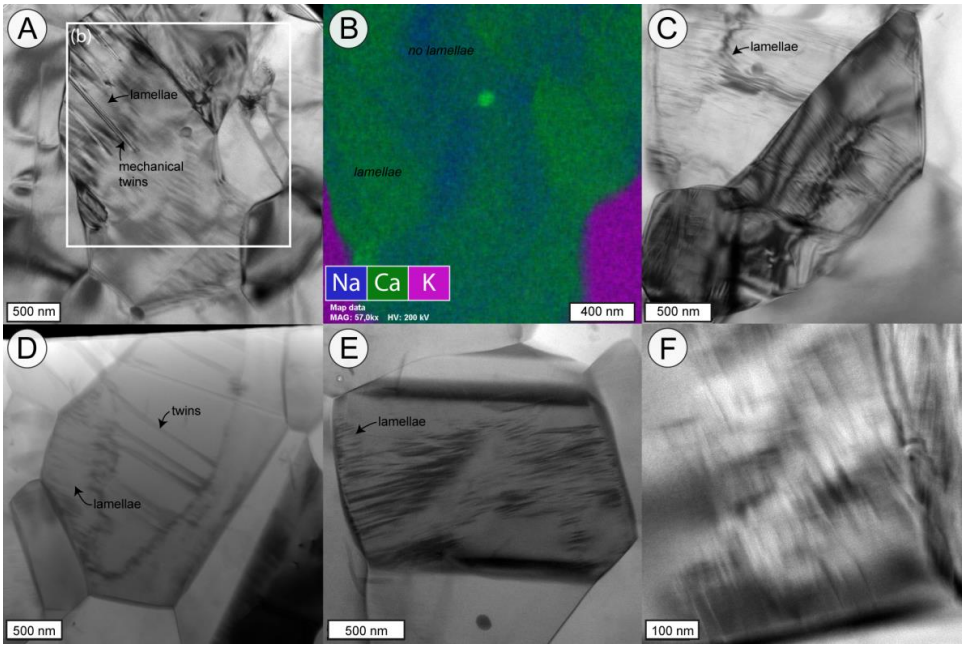

Figure 5: Plagioclase intergrowths in MF1. (a) BF-TEM image of the submicron lamellae in a plagioclase grains that are overlain by mechanical twins. **(b)** EDX map showing the distribution of Ca and Na in the plagioclase grains associated with the intergrowth in (a). The Ca-rich domains overlay the lamellae. **(c)** BF-TEM image of lamellae in two separate grains that show slight curvature. **(d)** BF-STEM image of discontinuous lamellae within a grain that hosts twins in its core. **(e)** STEM bright field image of discontinuous lamellae within a plagioclase grain. **(f)** Bright field TEM image of lamellae resembling 'tweed' exsolution within plagioclase.

https://doi.org/10.5194/se-2020-146
Preprint. Discussion started: 28 September 2020

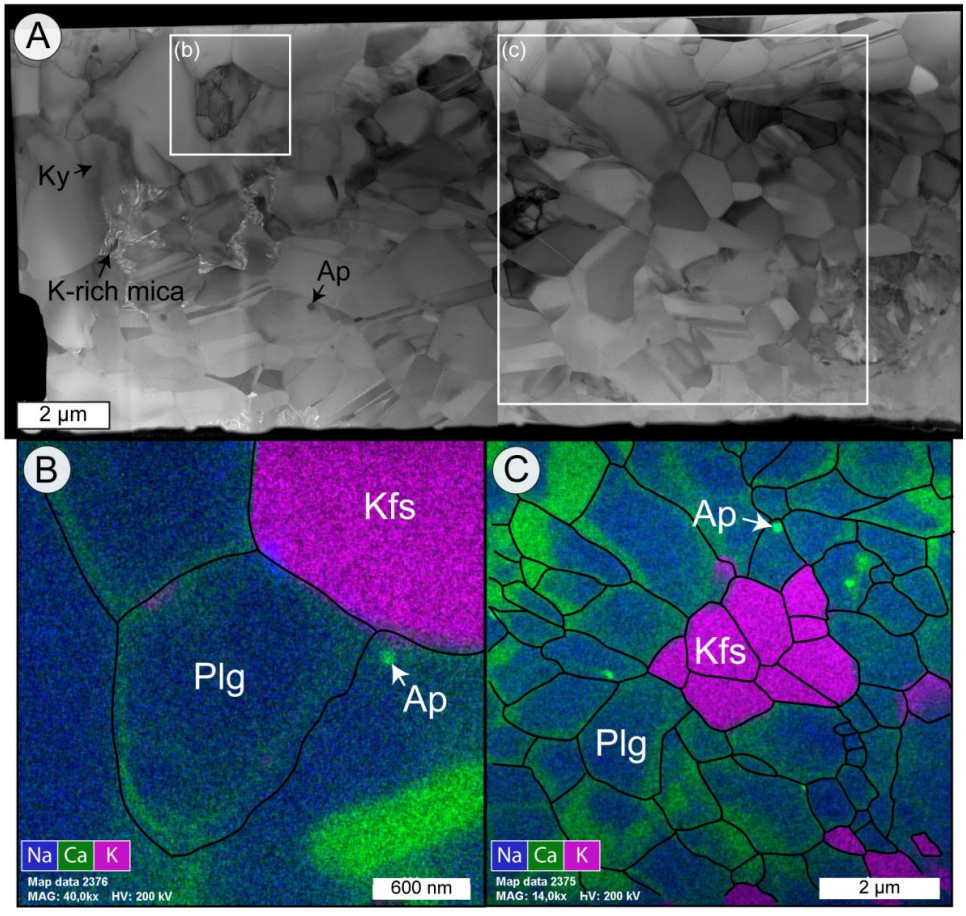

Figure 6: Microstructures of MF2. (a) Bright field image of the entire FIB cut from Fig. 1e. The plagioclase (Plg) microfracture contains dislocation-free grains with some twins. **(b)** EDX map of a dislocation-rich grain overlain with grain and phase boundaries (black). **(c)** EDX map of the area in (a) overlain with grain and phase boundaries (black). The Ca-rich domains are present along grain boundaries.